Mon. Not. R. Astron. Soc. **000**, 1–16 (2001) Printed 3 April 2002 (MN LaTeX style file v2.2)

Mass-to-light ratios from the fundamental plane of spiral galaxy disks

Alister W. Graham*
Instituto de Astrofísica de Canarias, La Laguna, E-38200, Tenerife, Spain

Accepted 2002 January 23

ABSTRACT

The best-fitting 2-dimensional plane within the 3-dimensional space of spiral galaxy disk observables (rotational velocity $v_{\rm rot}$, central disk surface brightness $\mu_0 = -2.5 \log I_0$, and disk scale-length h) has been constructed. Applying a three-dimensional bisector method of regression analysis to a sample of ∼100 spiral galaxy disks that span more than four mag arcsec^{-2} in central disk surface brightness yields $v_{\rm rot} \propto I_0^{0.50\pm0.05} h^{0.77\pm0.07}$ (B-band) and $v_{\rm rot} \propto I_0^{0.43\pm0.04} h^{0.69\pm0.07}$ (R-band). Contrary to popular belief, these results suggest that in the B-band, the dynamical mass-to-light ratio (within 4 disk scale-lengths) is largely independent of surface brightness, varying as $I_0^{0.00\pm0.10} h^{0.54\pm0.14}$. Consistent results were obtained when the expanse of the analysis was truncated by excluding the low surface brightness galaxies. *Previous claims that M/L_B varies with $I_{0,B}^{-1/2}$ are shown to be misleading and/or due to galaxy selection effects - not all low-surface-brightness disk galaxies are dark matter dominated.* The situation is however different in the near-infrared where $L_{K'} \propto v^4$ and $M/L_{K'}$ is shown to vary as $I_{0,K'}^{-1/2}$. *Theoretical studies of spiral galaxy disks should therefore not assume a constant M/L ratio within any given passband.*

The B-band dynamical mass-to-light ratio (within 4 disk scale-lengths) has no obvious correlation with $(B-R)$ disk colour, while in the K'-band it varies as -1.25±0.28$(B-R)$. Combining the present observational data with recent galaxy model predictions implies that the logarithm of the stellar-to-dynamical mass ratio is not a constant value, but increases as disks become redder, varying as 1.70±0.28$(B-R)$.

Key words: cosmology: dark matter – galaxies: fundamental parameters – galaxies: kinematics and dynamics – galaxies: photometry – galaxies: spiral

1 INTRODUCTION

Given the large observed range in the disk parameters of spiral galaxies, the tightness (and slope) of the Tully & Fisher (1977, hereafter TF) relation between absolute magnitude and the logarithm of the rotational velocity is a fundamental clue as to how these systems were constructed (Dalcanton, Spergel & Summers 1997; Mo, Mao & White 1998; Mo & Mao 2000; van den Bosch 2000; Koda, Sofue & Wada 2000; Bouwens & Silk 2002; Fall 2002). Not only does this relationship hold for the High Surface Brightness (HSB) spiral galaxies that typify the Hubble sequence, but also for the disk-dominated Low Surface Brightness (LSB) spiral galaxies (Zwaan et al. 1995). The universality of the TF relation for both HSB and LSB galaxies immediately tells us that for a given rotational velocity one has a constant galaxy luminosity, albeit within the scatter of the TF relation. This had been used to infer that, at any given constant luminosity, the mass-to-light (M/L) ratio must vary linearly with increasing disk scale-length h, or equivalently as $I_0^{-1/2}$, where I_0 is the central disk surface brightness in intensity units (Zwaan et al. 1995). Despite popular misconception, how the M/L ratio may vary between galaxies having different luminosities was not addressed by Zwaan et al. (1995) and is the subject of the present analysis.

Salucci, Ashman & Persic (1991) did investigate how M/L varies among galaxies having different luminosities and found $M/L_B \sim L_B^{-0.4}$. Their calculations were however performed under the belief that all disks have the same central surface brightness; indeed, much of their sample did. Contrary to this result, Karachentsev (1991) found M/L_B to be independent of luminosity for their galaxy sample. They deducted, as did Giovanardi & Hunt (1988), that M/L_B

* Present Address: Department of Astronomy, University of Florida, Gainesville, FL, USA

increased as the surface brightness decreased (that is, as the intensity decreased), which implies M/L_B must have increased as h increased for their sample. The goal of the present paper is to derive the mean dependency of the M/L ratio on both the scale-length and the (variable) central surface brightness of a galaxy's disk, rather than just one of these parameters.

The issue above is tackled by replacing the magnitude term in the TF diagram with the central disk intensity and scale-length terms (recall, $L_{\rm disk} = 2\pi I_0 h^2$). This gives three fundamental variables: the rotational velocity of the disk ($v_{\rm rot}$), the central disk surface brightness ($\mu_0 = -2.5 \log I_0$ mag arcsec^{-2}), and the disk scale-length (h). Just as the Faber-Jackson (1976) relation between absolute magnitude and velocity dispersion for Elliptical galaxies was supplemented through the construction of the 'Fundamental Plane' (Djorgovski & Davis 1987; Dressler et al. 1987; Faber et al. 1987), this study will explore the question of whether or not the use of three variables, rather than two are required for the treatment of spiral galaxy disks.

In recent years, numerous authors have addressed this question using different galaxy samples and different methods of data analysis (e.g., Willick et al. 1997). It should be noted that this question is approached here by treating all three variables equally (Feigelson & Babu 1992). It must therefore be understood that what is meant in the following text by 'departure from the TF relation' is a departure of the optimal 'fundamental plane' of spiral galaxy disks from the 'TF plane' when all three disk parameters are treated equally. Relations constructed for the purpose of galaxy distance determinations (see, for e.g., Triay, Lachieze-Rey & Rauzy 1994), where, typically, the residuals of only one variable about some relation are minimised are different; the results of such studies cannot be readily compared with the current investigation. Consequently, a number of such published data sets are reanalysed here in a consistent fashion. The tilt to the optimal 'fundamental plane' of spiral galaxy disks is subsequently used to infer the mass-to-light ratio as a function of disk scale-length and surface brightness.

Section 2 introduces the field galaxy samples that have been used, and the techniques employed to obtain their disk parameters. Section 3 describes the two-dimensional plane which is used to represent the location of galaxy disks in the three-dimensional space of observables, and describes how to relate this plane to the M/L ratio. The results and analysis of fitting such a plane to the data sample in hand is presented in section 4. The same method of analysis is then applied to various literature data samples, and extended to longer wavelengths through the study of a homogeneous sample of Cluster spiral galaxies for which B, R, I, and K' data is available. Lastly, a brief inspection of the M/L ratio dependency on disk colour is performed. The main results from this study are given in Section 6.

2 DATA

Three photometric samples have been compiled, containing galaxy profiles in both B- and R-bands. All these galaxies were then structurally modelled using the same algorithm. In order to cover a large range of disk parameters, the well-defined sample of morphologically undisturbed HSB galaxies from de Jong & van der Kruit (1994) and de Jong (1996) was used together with two large samples of LSB galaxies for which CCD data are available. The first of which is the sample of 21 disk-dominated LSB spiral galaxies from de Blok et al. (1995). The second is the sample of 21 bulge-dominated LSB spiral galaxies from Beijersbergen, de Blok & van der Hulst (1999).

The selection criteria are discussed at length in each paper, and they have been previously summarised in Graham & de Blok (2001). Briefly, de Jong & van der Kruit (1994) constructed a statistically complete, diameter- and volume-limited sample of 86 HSB disk galaxies having a red minor-to-major ratio greater than 0.625 (i.e. inclinations less than $\sim 50^{\rm o}$), and a red major-axis $\geq 2.0'$. Larger and brighter disk galaxies are of course over-represented in such a sample as they can be detected at greater distances; equivalently, small faint disks will be under-represented. Following McGaugh & Blok's (1998) study of LSB galaxies and the TF relation, the current objective is simply to expand the baseline of observable parameters which are fed into such an analysis. This HSB sample is therefore supplemented here with two LSB galaxy samples; however, as it turns out, the main conclusions from this study are supported by the analysis of the HSB data alone.

The first LSB sample is from de Blok et al. (1995), consisting of late-type LSB galaxies from van der Hulst et al. (1993) and the lists by Schombert & Bothun (1988) and Schombert et al (1992). De Blok et al. randomly selected a sub-set of galaxies with inclinations less than $60^{\rm o}$, central surface brightnesses fainter than 23 B-mag arcsec^{-2}, and having single-dish H$_{\rm I}$ observations available. The LSB sample from Beijersbergen et al. (1999) is a random selection of 'bulge-dominated' LSB disk galaxies imaged in the ESO-LV catalog (Lauberts & Valentijn 1989). Galaxies were selected if they had: inclinations less than $50^{\rm o}$, diameters of the 26 B-mag arcsec^{-2} isophote greater than $1'$ and smaller than $3'$ (chip size limitation), and a surface brightness of the disk at the half-light radii fainter than 23.8 B-mag arcsec^{-2}. The combined sample of HSB and LSB galaxies is not complete in any volume-limited sense, but does span more than 4 mag arcsec^{-2} in central disk surface brightness.

Every profile has been modelled by simultaneously fitting a seeing-convolved Sérsic (1968) $r^{1/n}$ bulge and a seeing-convolved exponential disk. Uncertainty in the relative sky-background level can be a significant source of error when determining the disk parameters; consequently, the parameters for the LSB galaxies ($\sim 1/3$ of the final sample) are less secure than those for the HSB galaxies. The LSB galaxies have typical errors of $\sim$20 per cent in their disk scale-length determinations, while the HSB galaxies generally have errors of less than 10 per cent (and typically 7 per cent). The profile derived central surface brightness measurements are accurate to typically 0.1 mag arcsec^{-2} for all galaxy types. They have also all been homogeneously corrected for: Galactic extinction (Schlegel, Finkbeiner & Davis 1998), K-correction (using the tables of Poggianti 1997), $(1+z)^4$ redshift dimming, and inclination corrected following the prescription Tully & Verheijen (1997) derived for the Ursa Major galaxy Cluster.

The inclination of each galaxy (determined from the R-band images) have been taken from their respective papers, with the exception that the inclinations given in de Blok, McGaugh & van der Hulst (1996) were used for the disk-dominated LSB galaxy sample. The galaxies have low to intermediate inclinations ($i<60°$). On the one hand, this is good because it means that the required surface brightness inclination corrections (to a face-on orientation) are small. Failing to account for such internal extinction can result in substantial errors – these can be greater than 2 mag for highly inclined disks. On the other hand, it means that the inclination corrections (to an edge-on orientation) for the rotational velocity terms will be large.

The 21 cm velocity data has come from a number of sources. The linewidth at 20 per cent of the peak HI intensity, denoted by W_{20} and usually measured to an accuracy of a few percent, has been used in all cases. Following Zwaan et al. (1995), these values were corrected for both inclination and random motion effects, as detailed in Tully & Fouqué (1985), to give the rotational velocity $v_{\rm rot}$. Dynamical data for the disk-dominated LSB galaxy sample has come from de Blok et al. (1996) and van der Hulst et al. (1993), and is thoroughly described in these papers. The data for the bulge-dominated LSB galaxies has come from de Blok (2001, priv. comm.) and was reduced in the same way as the disk-dominated sample of LSB galaxies. Measurements of W_{20} for the HSB galaxy sample have come from either the HI catalog of Huchtmeier (2000) or the database of LEDA. Uncertainties in the true inclination of each disk (due to possible intrinsic disk elongation) is likely to be the dominant source of error in the rotational velocity measurements and will contribute to scatter in the following diagrams. Adding an error estimate of 10° to every galaxies photometrically derived inclination angle resulted in a mean change of 0.09 dex in the derived rotational velocities. If more accurate inclinations derived from kinematical data (see, e.g., Franx & de Zeeuw 1992; Andersen et al. 2001) were available, one could expect the scatter in the following relations to be reduced. Similarly, rotation curve asymmetries have not been dealt with (Richter & Sancisi 1994; Haynes et al. 1994; Matthews & Gallagher 2002).

Considering galaxies with both photometric and kinematic data left a sample of 65 HSB and 30 LSB galaxies in the B-band, and 64 HSB and 31 LSB galaxies in the R-band (see Table 1). The galaxy F564-v3, the closest galaxy in the sample of disk-dominated LSB galaxies – at a distance of only 6 Mpc – is the only galaxy excluded at this point due to the uncertainty on its true distance[1].

[1] Inclusion of F564-v3 in the subsequent analysis reveals that it lies far from the relation defined by the other 94 galaxies in the sample; suggesting its distance is not well indicated by its redshift.

Table 1. Basic galaxy data

Galaxy Name	Morph. type (T)	Dist (Mpc)	b/a	$\mu_{0,B}$ mag arcsec^{-2}	$\log(h_B)$ (kpc)	$\mu_{0,R}$ mag arcsec^{-2}	$\log(h_R)$ (kpc)	W_{20} km s^{-1}
UGC 00242	7	56.9	0.77	—	—	19.781	0.529	271
UGC 00334	9	60.2	0.77	23.163	0.780	22.200	0.774	124
UGC 00438	5	58.7	0.78	20.459	0.600	19.289	0.591	372
UGC 00490	5	59.0	0.71	21.461	0.721	19.724	0.606	360
UGC 00508	2	60.7	0.89	21.422	0.865	19.686	0.797	488
UGC 00628	9	70.6	0.63	22.670	0.676	21.676	0.653	228
UGC 01305	4	35.7	0.81	21.593	0.705	20.206	0.703	329
UGC 01551	8	36.0	0.89	22.147	0.653	21.008	0.624	132
UGC 01577	4	69.1	0.79	21.620	0.759	20.232	0.749	287
UGC 01719	3	107.6	0.74	22.163	1.029	20.688	0.982	505
UGC 02064	4	56.5	0.70	21.873	0.741	20.517	0.703	263
UGC 02124	0	35.7	0.88	22.127	0.569	20.637	0.608	181
UGC 02368	3	48.0	0.92	21.142	0.568	19.822	0.512	385
UGC 02595	4	78.3	0.78	—	—	20.104	0.815	276
UGC 03080	5	49.5	0.91	21.825	0.661	20.397	0.570	170
UGC 03140	5	63.8	0.94	20.690	0.616	—	—	145
UGC 04126	3	70.2	0.85	21.436	0.820	20.024	0.764	295
UGC 04256	5	75.3	0.86	21.084	0.856	—	—	205
UGC 04308	5	54.1	0.77	21.191	0.701	20.041	0.665	263
UGC 04368	6	58.1	0.80	21.387	0.681	20.263	0.654	248
UGC 04375	5	34.5	0.66	21.190	0.516	19.990	0.476	295
UGC 04422	4	66.1	0.82	21.978	1.004	20.657	0.968	376
UGC 04458	1	69.5	0.87	22.784	0.978	21.239	0.940	285
UGC 05103	3	57.3	0.61	20.494	0.673	19.492	0.616	398
UGC 05303	5	24.8	0.59	21.207	0.592	20.069	0.547	294
UGC 05510	4	24.9	0.81	20.609	0.385	19.577	0.348	187
UGC 05554	1	23.9	0.69	21.022	0.341	19.654	0.298	284
UGC 05633	8	25.9	0.63	22.967	0.523	21.978	0.545	177
UGC 05842	6	22.4	0.85	21.815	0.743	20.617	0.602	166
UGC 06077	3	26.9	0.82	20.959	0.371	19.738	0.348	142
UGC 06277	5	15.7	0.88	20.890	0.333	19.730	0.284	134
UGC 06445	4	24.5	0.84	20.562	0.294	19.159	0.228	184
UGC 06453	4	23.5	0.75	20.328	0.279	—	—	241
UGC 06460	4	23.4	0.75	20.609	0.474	19.569	0.450	202
UGC 06693	4	99.5	0.85	21.571	0.947	20.273	0.894	189
UGC 06746	0	99.2	0.76	21.406	0.921	20.355	0.959	551
UGC 06754	3	101.3	0.89	23.140	1.332	21.068	1.103	224
UGC 07169	5	36.3	0.81	19.827	0.343	18.613	0.263	227
UGC 07315	4	09.2	0.67	20.037	-0.17	18.878	-0.164	250
UGC 07450	4	29.0	0.89	21.038	0.935	19.782	0.912	268
UGC 07523	3	12.3	0.81	21.143	0.279	19.869	0.241	178
UGC 07594	2	33.9	0.69	21.305	0.970	20.063	0.963	306
UGC 07901	5	08.8	0.67	19.746	-0.060	18.377	-0.142	384
UGC 08289	4	53.2	0.89	21.711	0.940	20.244	0.781	243
UGC 08865	2	38.6	0.76	21.753	0.733	20.666	0.730	302
UGC 09061	4	79.9	0.91	22.547	1.360	21.174	1.274	195
UGC 09481	4	56.4	0.74	21.270	0.688	20.122	0.650	243
UGC 09926	5	30.8	0.71	19.945	0.421	—	—	351
UGC 09943	5	30.7	0.64	20.207	0.451	19.284	0.460	326
UGC 10083	2	28.7	0.82	20.791	0.391	19.428	0.335	178
UGC 10445	6	15.1	0.78	21.994	0.280	21.040	0.173	159
UGC 10584	5	73.0	0.88	21.837	0.915	20.539	0.852	261
UGC 11628	2	55.6	0.70	22.467	1.124	20.646	0.952	503
UGC 11708	5	54.6	0.81	21.249	0.661	20.039	0.663	297
UGC 11872	3	15.7	0.74	21.015	0.222	19.032	0.129	312
UGC 12151	10	23.0	0.87	22.822	0.414	21.981	0.361	180
UGC 12343	5	31.0	0.77	21.023	0.767	19.800	0.766	376
UGC 12379	4	80.6	0.91	21.792	0.886	20.326	0.893	308
UGC 12391	5	62.9	0.89	21.312	0.685	20.071	0.665	216
UGC 12511	6	45.9	0.82	22.282	0.712	20.685	0.567	278
UGC 12614	5	45.0	0.74	20.816	0.657	19.609	0.636	315
UGC 12638	5	72.7	0.81	21.913	0.861	20.615	0.830	303
UGC 12654	4	52.1	0.82	21.519	0.684	20.340	0.655	237

Redshifts for ESO-LV 0350110 and ESO-LV 0050050, from the bulge-dominated sample of LSB galaxies, were obtained from the Parkes telescope HIPASS database (Barnes et al. 2001). Redshifts for the other galaxies have been taken from the NASA/IPAC Extragalactic Database (NED). The heliocentric redshifts were uniformly corrected for Galactic rotation, Virgo-infall, infall toward the 'Great Attractor', and the 'local anomaly' using the model from Burstein et al. (1989). The disk scale-lengths were then converted from arcseconds to kpc using a Hubble constant $H_0 = 75$ km s^{-1} Mpc^{-1}.

In passing, it is noted that the sample of galaxies has been taken from the field, rather than from a single cluster, and so one can expect to have a greater degree of scatter in the relationship between $\log v$, μ_0, and $\log h$ than might otherwise be attained. This is because peculiar velocity flows leading to distance errors will introduce errors into the estimates of the scale-lengths. Additionally, like most studies to date, W_{20} has been used to derive $v_{\rm rot}$ rather than using v_{max} or $v_{\rm flat}$ which are not available. It is acknowledged that the available kinematic data may therefore not be the optimal estimate to the rotational velocity, although McGaugh & de Blok (1998) state that W_{20} gives a good approximation to $v_{\rm flat}$.

3 THE RELATION BETWEEN $\log v$, μ_0 AND $\log h$, AND IMPLICATIONS FOR THE M/L RATIO

From the balance of forces between centripetal acceleration and gravity, one has the dynamical mass $M(r) = v^2 r/G$, where G is the gravitational constant. Combining this with the previous expression for L (Section 1) gives

$$\frac{M}{L} \propto \frac{v^2 r}{I_0 h^2}, \tag{1}$$

where M and v are measured at the same radius r. A common practice is to take r as some multiple of h (e.g. $4h$, McGaugh & de Blok 1998) and assume the estimate of v derived from W_{20} is a good estimate of not only $v_{\rm flat}$ (McGaugh et al. 2000) but also of the rotational velocity at $4h$. Doing this, one arrives at the virial theorem

$$v^2 \propto (M/L) I_0 h. \tag{2}$$

Next, from the measured data of many galaxies, one can construct – given it exists – the 'plane'

$$v \propto I_0^x h^y, \tag{3}$$

where x and y are the optimal exponents dictating the relationship between the disk's structural and dynamical terms. Combining equations 2 and 3 to eliminate the velocity term, one quickly arrives at the relation

$$-2.5 \log \frac{M}{L} \propto (2x-1)\mu_0 - 2.5(2y-1)\log h. \tag{4}$$

Subsequently, lines of constant M/L will have a slope of $2.5(2y-1)/(2x-1)$ in the μ_0–$\log h$ diagram (e.g. Graham & de Blok 2001). One can similarly derive that lines of constant velocity have a slope of $2.5y/x$.

If the value of $v_{\rm rot}$ derived from W_{20}, or $v_{\rm flat}$, is an appropriate velocity to use at some constant multiple of h (e.g. $4h$), and galaxy disks are virialised, then the M/L ratio derived in equation 4 should be proportional to the M/L ratio derived from

$$M/L \mid_{4h} \propto v^2 4h/(I_0 h^2). \tag{5}$$

I shall refer to this as the 'kinematical' or 'dynamical' mass-to-light ratio, and that in equation 4 as the 'photometric' mass-to-light ratio.

What M/L ratio does one really want to measure? Lets start by looking at the different ways which can be used to measure L. The flux within some limiting isophotal radius is clearly inappropriate. This is strikingly evident in the case of LSB galaxies whose central surface brightness values may be fainter than the limiting isophotes used to measure the HSB galaxies. In such an instance, the flux measurement of the LSB galaxy would be zero. The use of the outer most observed radius is also not ideal because it depends on observational details such as exposure times, telescope aperture, and what signal-to-noise one is willing to accept; that is, the outer most observed radius is not an intrinsic quantity of a galaxy. Another way to estimate the luminosity of galaxies is to measure their flux within some fixed aperture size, say 20 kpc. Although this is indeed a standard and consistent approach, it is again not a favourable one. The reason is because, depending on μ_0 and h, *this metric will measure a different fraction of the total galaxy luminosity.* Given that exponential disks are structurally homologous, scaling with the central intensity and scale-length, one can, and indeed should, use these quantities to measure the same fraction of disk light for all galaxies (for example, 91 per cent of the light from an exponential profile which extends to infinity is contained within the inner four scale-lengths; 99.1 per cent within the inner 4 effective radii). Therefore, some constant multiple of $I_0 h^2$ will represent the same fraction of the total extrapolated disk light for all disks. Disk truncation in real galaxies at 4 or more scale-lengths will introduce less than a 10 per cent error to this approach.

What about the estimate for the mass M? One could also measure the galaxy mass within 20 kpc, or within a fixed number of disk scale-lengths. But is this really what we want? If the total (stars + gas + dark matter) mass profile does not scale with the luminous disk scale-length, then estimates of the galaxy mass within a fixed number of disk scale-lengths from different galaxies will not correspond to equal fractions of their mass distribution. Therefore, a more fundamental quantity might be the mass within some constant multiple of the core-radii of the *total* mass profile, defined to be the radius where the density has dropped by a factor of two from its central value. If the mass profiles are homologous, then the mass would simply scale with some measure of velocity and some measure of radius. The presence of the flat rotation curves suggests a velocity scale we can use, namely $v_{\rm flat}$. This then leaves the radial scale-size to be determined, and one typically assumes that the scale-size 'a' of the *total* mass profile, scales with the disk scale-length (McGaugh & de Blok 1998)[2]. If they do not, then one should add the term $-2.5\log(a/h)$ to the right hand side of equation 4.

[2] Alternative scales could be the velocity v_0 at the radius r_0 from the density profiles used in Kravtsov et al. (1998).

Table 1. – *continued*

Galaxy Name	Morph. type (T)	Dist (Mpc)	b/a	$\mu_{0,B}$ mag arcsec^{-2}	$\log(h_B)$ (kpc)	$\mu_{0,R}$ mag arcsec^{-2}	$\log(h_R)$ (kpc)	W_{20} km s^{-1}
UGC 12732	9	11.4	0.89	—	—	21.515	0.087	127
UGC 12754	6	11.5	0.70	21.231	0.370	20.207	0.321	206
UGC 12776	3	64.1	0.88	23.305	1.355	21.834	1.149	256
UGC 12808	3	54.4	0.93	19.839	0.503	18.659	0.504	362
F561-1	9	70.1	0.91	22.738	0.478	21.843	0.437	069
F563-1	9	53.9	0.91	23.716	0.730	22.602	0.628	115
F563-V1	10	59.5	0.500	23.669	0.450	22.358	0.432	097
F563-V2	10	64.5	0.88	22.061	0.368	—	—	132
F564-v3	10	05.9	0.87	23.824	-0.519	22.890	-0.588	065
F565-V2	10	56.7	0.50	24.065	0.463	23.394	0.438	126
F567-2	9	83.5	0.94	23.995	0.692	22.936	0.577	074
F568-1	5	94.1	0.90	23.617	0.775	22.619	0.710	150
F568-3	7	86.1	0.77	22.571	0.575	21.611	0.528	180
F568-V1	7	84.5	0.77	22.741	0.484	21.942	0.466	176
F571-5	9	65.1	0.77	23.362	0.496	22.647	0.448	179
F571-V1	7	84.2	0.82	23.590	0.511	22.637	0.472	084
F5741-	7	99.2	0.42	—	—	22.386	0.749	223
F574-2	9	91.9	0.88	24.102	0.754	23.027	0.635	068
F577-V1	7	103.7	0.82	23.787	0.799	23.046	0.718	094
F583-1	9	35.1	0.45	23.012	0.318	22.234	0.275	183
UGC 1230	9	50.4	0.94	23.208	0.677	22.333	0.609	115
UGC 128	8	58.9	0.55	23.405	0.864	22.488	0.764	214
UGC 6614	1	92.1	0.59	—	—	22.567	1.114	262
1150280	5	88.2	0.62	20.772	0.657	19.639	0.640	190
1530170	4	88.3	0.71	—	—	21.369	0.941	198
2520100	3	130.9	0.76	23.894	1.406	21.106	0.929	434
0350110	1	86.1	0.77	20.829	0.690	19.529	0.648	285
3740090	1	41.8	0.81	22.704	0.428	21.145	0.374	076
4220090	7	65.9	0.91	22.901	0.717	21.796	0.589	078
4250180	7	95.1	0.84	23.378	0.945	21.932	0.821	101
4990110	7	41.0	0.83	22.738	0.423	21.995	0.498	090
0050050	8	77.2	0.92	22.453	0.705	21.454	0.621	132
0540240	2	198.7	0.84	23.555	1.111	22.289	1.012	399
5520190	2	159.5	0.62	22.488	1.115	20.810	0.942	459
0590090	8	18.4	0.88	21.847	0.283	20.812	0.262	053
1220040	1	127.0	0.63	23.272	1.227	21.213	0.882	101

Column 1 gives the galaxies identification. The HSB sample from de Jong & van der Kruit (1994) are designated according to their UGC number; the LSB galaxies from de Blok et al. (1995) which are labelled F (except for 3 galaxies labelled with a UGC number) are from the lists of Schombert et al. (1992); the LSB galaxies from Beijersbergen et al. (1999) are denoted simply with a numeric code which refers to the ESO-LV number from the catalog of Lauberts & Valentijn (1989). The galaxy type, or numerical stage index T (de Vaucouleurs et al. 1991), is given column 2. Column 3 gives the galaxy distance in Mpc (assuming $H_0 = 75$ km s^{-1} Mpc^{-1}) after correcting the observed redshift (courtesy of NED) for Galactic rotation, Virgo-infall and infall towards the 'Great Attractor' using the model and code from Burstein et al. (1989). Column 4 gives the (R-band) axis-ratio of each disk. The central B-band disk surface brightness and disk scale-length are given in Columns 5 and 6. The surface brightness term has been corrected for the various effects described in Section 2 of the text. Column 7 and 8 are the R-band equivalent of Column 5 and 6. Column 9 gives the observed linewidth at 20 per cent of the peak HI intensity.

Whether or not galaxy rotation curves are homologous appears to be something of an unresolved question (van den Bosch et al. 2000; see also Rubin et al. 1985, Persic & Salucci 1991 and Salucci & Borriello 2002). Swaters, Madore & Trewhella (2000; their figure 4) present H_α rotation curves for a small sample of LSB and HSB galaxies which appear to overlay each other exactly (once normalised with $v_{\rm flat}$ and h). This contradicts the work of de Blok & McGaugh (1997) and suggests that a/h may be constant. Most recently, fitting pseudo-isothermal mass models (in preference to Navarro, Frenk & White (1996) CDM halos), de Blok, McGaugh & Rubin (2001; their figure 10) studied a sample of well-resolved LSB galaxy rotation curves and found no appreciable evidence for any correlation between a/h and the maximum rotational velocity, or equivalently luminosity.

In what follows, the additional term a/h will be ignored and the kinematical M/L ratio shall be that within 4 scale-lengths, as defined in equation 5.

If the TF relation is indeed the optimal representation of disk galaxies, then one must find from equation 3 that

y=2x and $v \propto L^x$. The exact slope of the TF relation is important because it tells us the M/L dependency on the other galaxy parameters. For example, if $L \propto v^2$ (x=0.5, y=1.0) then $(M/L) \propto h$ and is independent of surface brightness.[3] However, if $L \propto v^4$ (x=0.25, y=0.5) then $(M/L) \propto 1/\sqrt{I_0}$, independent of galaxy size.

In the original paper of Tully & Fisher (1977), they found a slope of 2.5±0.3 using photographic magnitudes and the velocity line width at 20 per cent of the maximum intensity. More recently, Zwaan et al. (1995) obtained a B-band slope of 2.6, implying that $\log(M/L_B) \propto (0.09\mu_0 + 0.54\log h)$[4] This result is not at odds with the conclusion of Zwaan et al. (1995) that $M/L \propto I_0^{-1/2}$, because their statement only holds valid, as they state, for galaxies of a fixed/constant luminosity. This point has, however, not always been appreciated in the literature.

Let us consider the case where $L \propto v^2$ and $\log(M/L) \propto \log h$, independent of μ_0. If one was to sample different galaxies having the same h but different μ_0, $\log(M/L)$ would show no dependency at all on μ_0. If one was to then sample a different set of galaxies having equal luminosity, but with different μ_0 and h, a plot of $\log(M/L)$ versus μ_0 would of course show a strong correlation This is because of the relation between μ_0 and h at constant L. One must therefore be careful of misleading results of this kind. Completely independently of any observational results, one can see this degeneracy at constant L by dividing the relation $M \propto v^2 h$ by L to give $(M/L) \propto v^2 h/L$. If the TF relation holds true with any slope at all, then one has that $(M/L) \propto h$ for any fixed L. *Of course, for different values of L the constant of proportionality between M/L and h is different (unless $L \propto v^2$) and so one cannot use this expression to compare the M/L ratios between galaxies of different luminosity, only between galaxies of the same luminosity.* Alternatively, Zwaan et al. (1995) showed that $I_0(M/L)^2$ is constant at any fixed linewidth (or, from the TF relation, any fixed luminosity); therefore, $(M/L) \propto 1/\sqrt{I_0}$. However, if $I_0 h^2$ is constant, one again has that $(M/L) \propto h$. Identically, *one cannot use the relation $(M/L) \propto 1/\sqrt{I_0}$ to compare the M/L ratio of galaxies at different luminosities (unless $L \propto v^4$)*. Only for galaxies having the same fixed luminosity can these expressions be used to indicate differences in the M/L ratio. How the M/L ratio of galaxies *with different luminosities* varies (simultaneously) with scale-length and the central disk intensity is what this study shall investigate.

4 ANALYSIS AND RESULTS

A Principle Component Analysis was performed on the data, revealing that 95 per cent (B-band) and 94 per cent (R-band) of the variance within the 3-dimensional space of variables (μ_0, $\log h$, $\log v$) resides within a two-dimensional plane[5]. From this it is concluded that it is indeed appropriate to represent the data with a two-dimensional plane.

[3] This result actually holds for any value of y as long as x=0.5.
[4] n.b. Along lines of constant luminosity in the μ_0–$\log h$ diagram, if $\log(M/L) \propto 0.1\mu_0 + 0.5\log h$ then it implies that both μ_0 and $\log h$ contribute equally to changes in M/L.
[5] The principle eigenvector accounted for 49 per cent (B-band) and 55 per cent (R-band) of the variance.

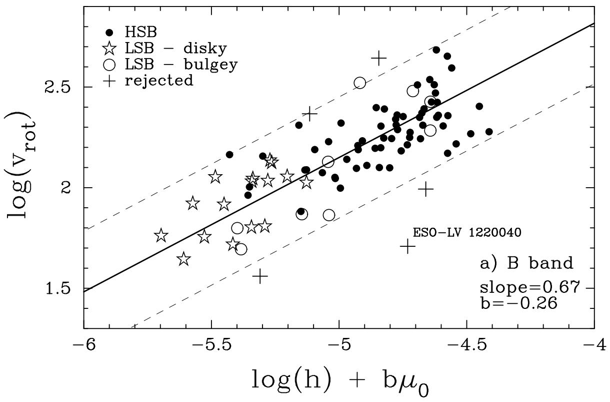

Figure 1. Correlation between the dynamical and structural properties of spiral galaxy disks. The 'mixing' value b (see, e.g., Djorgovski & Davis 1987) is chosen such that it yields the highest linear correlation coefficient between $\log v_{\rm rot}$ and $(\log h + b\mu_0)$. The solid line represents the best fit from an orthogonal regression analysis, and the dashed lines mark the boundary which is a factor of 2 away in $v_{\rm rot}$ from the line of regression. The different symbols denote from which galaxy sample the data are from: filled circles represent galaxies from the sample of de Jong & van der Kruit (1994), stars are for galaxies from de Blok et al. (1995), open circles are for galaxies from Beijersbergen et al. (1999), and the plus signs denote the five outlying points which have been rejected from the analysis. The perpendicular scatter in both panels a) B-band and b) R-band is 0.11 dex.

In so doing, five galaxies (3 LSB and 2 HSB) from the final sample of 94 have been identified as potential outliers – one in particular (ESO-LV 1220040). The following analysis has therefore been performed excluding ESO-LV 1220040, and then performed again excluding all five galaxies, which, in a number of tests, consistently lied away from the main data. These points are shown in Figure 1 – identified as lying more than a factor of 2 in $v_{\rm rot}$ from the best-fitting line to the data sample. Two[6] of these galaxies have an inclination of $\sim 25°$, and another is the closest galaxy from the HSB sample – having a redshift of only 800 km s^{-1}. The above percentages increased by 1 per cent, to 96 per cent (B-band) and 95 per cent (R-band), when all five outlying data points were excluded.

To construct the best-fitting plane, a three-dimensional bisector method of linear-regression was used (Graham & Colless 1997). The advantages and applicability in treating all the variables equally in this manner, as opposed to a simple linear regression of one variable on the others, is elucidated in Isobe et al. (1990) and Feigelson & Babu (1992). Basically, one wants to treat all the data/variables in an equivalent manner when performing a comparison with theory. A simple ordinary linear regression (OLS) of one variable on the other two variables would not achieve this goal, and would produce different results depending on which variable one regressed upon the others. Of those methods which do provide a symmetrical treatment of the data, the bisector method provides the smallest variance, or uncertainty, to the estimated values of the fitted plane.

Performing this regression, the exponents x and y

[6] An additional 10 galaxies have inclinations <25°, but all closely follow the relation defined by the other galaxies.

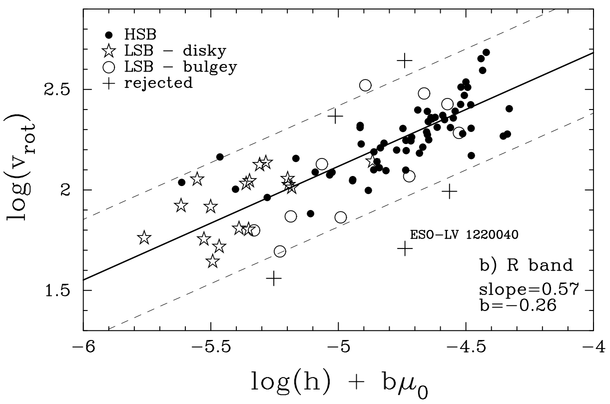

Figure 1 – *continued*

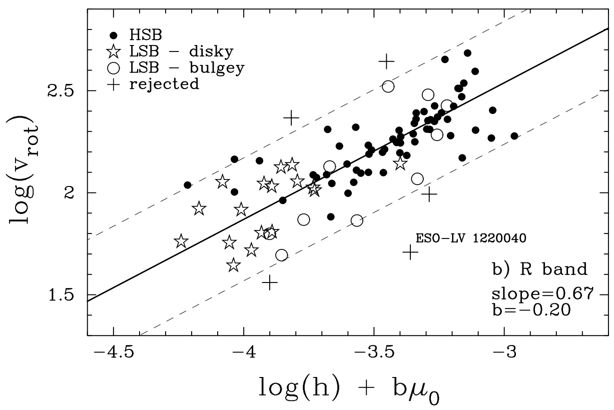

Figure 2 – *continued*

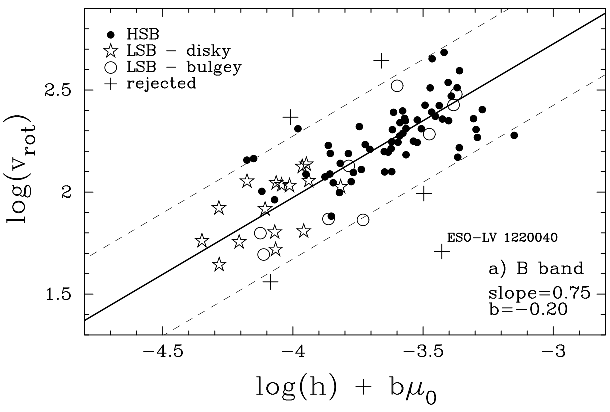

Figure 2. Same as Figure 1a and 1b, except that the value of b has been fixed equal to -0.2 to mimic the TF relation, where $L \propto v^{\alpha}$ and α is obtained here by dividing 2.0 by the slope of the fit. The perpendicular scatter in both panels a) B-band and b) R-band is 0.11 dex.

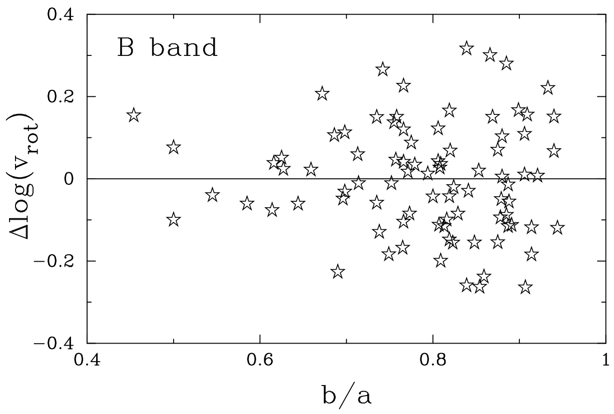

Figure 3. The vertical residuals about the best-fitting line in Figure 1a are plotted against a) each galaxies observed minor-to-major axis ratio (b/a), and b) the $B-R$ colour of each disk.

from equation 3 were computed to be 0.53±0.05 and 0.79±0.09 (B-band) and 0.45±0.04 and 0.71±0.09 (R-band). Therefore, $(M/L_B) \propto I_0^{0.06\pm0.10} h^{0.58\pm0.18}$ (B-band) and $(M/L_R) \propto I_0^{-0.10\pm0.08} h^{0.42\pm0.18}$ (R-band). Lines of constant velocity subsequently have a slope of $2.5y/x = 3.7\pm0.5$ (B-band) and 3.9±0.6 (R-band) in the μ_0–$\log h$ diagram. A plot of $\log v$ against $\log(I_0^x h^y)$ does, as one would hope, have a slope of 1. This figure is not presented here because it is attained by simply dividing the x-axis in Figure 1 by the slope of that data. Therefore, a scaled version of such a plot is already displayed. Both of the TF relations shown in Figure 2 (obtained by setting the 'mixing' value $b \equiv -x/(2.5y) = -0.2$) have a vertical scatter of 0.14 dex, slightly greater than the value 0.13 dex (c.f. 0.65 mag, Kannappan, Fabricant & Franx 2002) obtained in Figure 1.

The above analysis was repeated, removing those *additional* four data points marked as outliers in Figure 1. This time x=0.50±0.05 and y=0.77±0.07 (B-band), and x=0.43±0.04 and y=0.69±0.07 (R-band). Here, $(M/L_B) \propto I_0^{0.00\pm0.10} h^{0.54\pm0.14}$ (B-band) and $(M/L_R) \propto I_0^{-0.14\pm0.08} h^{0.38\pm0.14}$ (R-band), and lines of constant velocity have a slope of 3.9±0.5 (B-band) and 4.0±0.6 (R-band) in the μ_0–$\log h$ diagram. At least in the B-band, the data reveal that the M/L ratio is in fact largely independent of surface brightness, and roughly varies as $\sqrt{h}$. *Lower surface brightness does not necessarily imply a higher M/L ratio.* The residuals are shown not to correlate with either $(B-R)$ colour (Figure 3), or galaxy ellipticity, and hence no obvious additional dependency on inclination is expected. Studies which explore the density profiles of dark matter halos associated with LSB galaxies should perhaps reconsider the assumption that all of these systems are dark matter dominated.

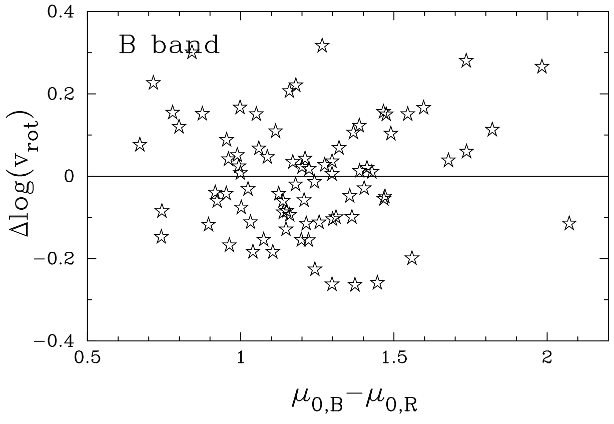

Figure 3 – *continued*

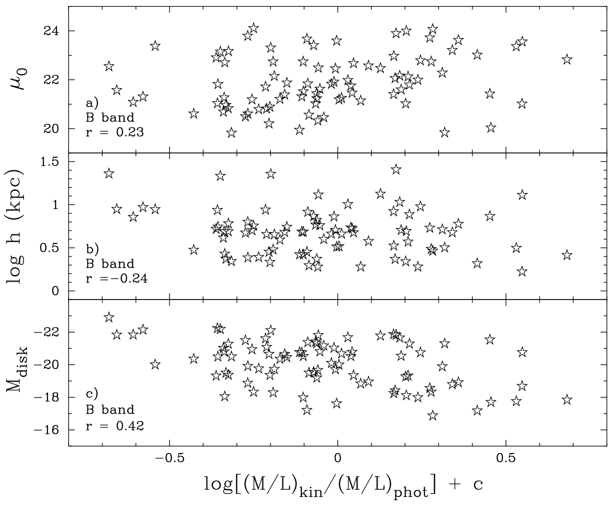

Figure 4. The logarithm of the difference between the mass-to-light ratio estimates obtained using equation 4 and equation 5 have been plotted against a) the central disk surface brightness, b) the logarithm of the disk scale-length, and c) the absolute magnitude of the disk. No strong trends exists. These plots show the B-band data, excluding the 5 outlying points identified in Figure 1. The values for x and y used in equation 4 have been taken to be 0.50 and 0.77. Constants of proportionality have been ignored; the constant c in the x-axis is the same for all galaxies.

Differences in the mass-to-light ratios estimated from equation 4 and equation 5 may signify that galaxies are either not virialised or that the mass profiles do not scale simply with the luminous exponential disk scale-length (section 3). The logarithm of the ratio of the 'kinematic' and 'photometric' mass-to-light ratios has been plotted against the central disk surface brightness, the logarithm of the luminous disk scale-length, and the logarithm of the disk luminosity in Figure 4. No strong correlations exist, although a weak correlation (Pearson's $r = 0.4$) with absolute magnitude does exist at the 99.97 per cent confidence level. This may be indicating that the ratio of the mass profile scale-size (a) to the (B-band) luminous disk scale-length (h) may correlate weakly with luminosity, in the sense that a/h decreases with increasing disk luminosity.

One way to test if the above trend is true would be from an analysis of actual rotation curves. If rotation curves are homologous, scaling in amplitude with $v_{\rm flat}$ and radially with disk scale-length h, then they should all overlap each other once normalised in this way. However, because rotation curves can rise slowly as they approach $v_{\rm flat}$ (see, for e.g., Rubin et al. 1985), it is difficult to quantify at exactly which radius $v_{\rm flat}$ is reached. It can therefore be difficult to gauge if rotation curves are homologous. It is proposed here that one might be able to use the radius where the velocity equals one-half of $v_{\rm flat}$ as a measure of the radial scale for the velocity profile. Due to the relative steepness of rotation curves around this value (after they have been scaled with the disk scale-length), errors in $v_{\rm flat}$ should have a reduced effect on estimates of this radius. A plot of this radius, in units of disk scale-length, against disk luminosity may reveal if the assumption that the mass profiles scale with the luminous disk profiles is valid, or if the slight correlation found above is real.

4.1 Further analysis

A range of methods have been used in the literature for the task of constructing a two-dimensional plane to three-dimensional data. Given the lack of universal agreement as to which is the best approach to take, a second (different) approach is employed here. Following Djorgovski & Davis (1987), the 'mixing' value b that gave the highest linear correlation coefficient between $\log v$ and $(\log h + b\mu_0)$ was computed. A line of regression to this two-parameter data set (once the value of b had been determined) was then fitted; in fact, six different lines of regression were fitted using the program SLOPES from Feigelson & Babu (1992). The results are given in Table 2, and were obtained excluding the 1 outlying data point (ESO-LV 1220040). Through a bootstrap resampling of the data an estimate for the error on b was obtained and is also given in Table 2. When all five outlying data points were excluded, $b{=}-0.256 \pm 0.030$ (B-band) and $b{=}-0.265 \pm 0.036$ (R-band), in agreement with the results obtained in Table 2. Again, the analysis and data suggests that in the B-band $x \sim 0.5$ and the M/L_B ratio is largely independent of surface brightness. Once more, only mild inconsistencies with the TF expectation value of $b = -0.2$ were found using this alternative technique to compute the best-fitting plane. Within the 2σ confidence interval, the optimal values of b are consistent with the value -0.20. Forcing the value of b to equal -0.20 introduced a slight dependency of M/L on the surface brightness term – as evidenced by the departure of x from the value 0.5 in Table 2. The extent of this effect was greater in the redder passband.

A significant fraction (1/2) of the LSB galaxies have rotational velocity estimates less than 100 km s^{-1}. In order to obtain an estimate as to how the LSB galaxies may be influencing the above results, the analysis was repeated using the HSB galaxy sample on their own, and then again using only the LSB galaxy sample. Excluding the outliers identified in Figure 1, the three-dimensional bisector method of regression for the HSB galaxy sample ($N = 62, 61$) gave $v \propto I_0^{0.60\pm0.12} h^{0.82\pm0.12}$ (B-band) and $v \propto I_0^{0.50\pm0.09} h^{0.66\pm0.09}$ (R-band).[7] One can therefore conclude that the LSB galaxies are not responsible for the observed, albeit slight, departures from the TF relation, nor are they biasing the analysis to produce values of x as high as 0.5 and thereby causing the M/L ratio to appear largely independent of surface brightness. The regression analysis of the LSB galaxy sample ($N = 25, 27$) gave $v \propto I_0^{0.58\pm0.17} h^{0.92\pm0.15}$ (B-band) and $v \propto I_0^{0.46\pm0.17} h^{0.79\pm0.18}$ (R-band), fully consistent with the result from the HSB galaxy sample. The reason for the slightly larger exponents when the HSB and the LSB galaxies are considered on their own, as opposed to taken together, can be easily understood by looking at the distribution of LSB and HSB galaxies in Figure 1. This slight difference in slopes also illustrates how a selection bias against LSB galaxies would operate; removing the left half of the data in Figure 1 results in an increased slope in the best-fit to the remaining data (see, e.g., Lynden-Bell et al. 1988, Appendix B).

A remaining point of concern is that there may be rela-

[7] From the second method of analysis, the 'mixing' values were determined to be $b{=}0.244{\pm}0.044$ (B-band) and $b{=}0.260{\pm}0.050$ (R-band).

Table 2. Regression analysis: Field Galaxies

method	intercept	slope ($=y$)	$x=-2.5\times b\times y$
B-band: b=-0.265 ± 0.034			
OLS(Y|X)	5.149±0.267	0.576±0.052	0.382±0.053
OLS(X|Y)	7.158±0.417	0.967±0.081	0.641±0.086
OLS bisector	6.060±0.270	0.753±0.052	0.499±0.063
Orthogonal	5.719±0.330	0.687±0.064	0.455±0.064
Reduced major axis	6.024±0.276	0.747±0.054	0.495±0.063
Mean OLS	6.153±0.286	0.772±0.056	0.511±0.065
B-band: b=-0.200			
OLS(Y|X)	4.539±0.240	0.633±0.065	0.317±0.033
OLS(X|Y)	6.321±0.347	1.112±0.093	0.556±0.047
OLS bisector	5.326±0.225	0.844±0.060	0.422±0.030
Orthogonal	5.134±0.298	0.793±0.080	0.397±0.040
Reduced major axis	5.305±0.234	0.839±0.063	0.420±0.032
Mean OLS	5.430±0.238	0.872±0.064	0.436±0.032
R-band: b=-0.278 ± 0.040			
OLS(Y|X)	4.754±0.235	0.499±0.046	0.347±0.055
OLS(X|Y)	6.434±0.360	0.825±0.071	0.573±0.089
OLS bisector	5.532±0.244	0.650±0.048	0.452±0.067
Orthogonal	5.127±0.284	0.571±0.056	0.397±0.065
Reduced major axis	5.489±0.248	0.642±0.049	0.446±0.067
Mean OLS	5.594±0.256	0.662±0.050	0.460±0.069
R-band: b=-0.200			
OLS(Y|X)	4.230±0.208	0.580±0.059	0.290±0.030
OLS(X|Y)	5.727±0.294	1.003±0.084	0.502±0.042
OLS bisector	4.902±0.201	0.770±0.058	0.385±0.029
Orthogonal	4.663±0.258	0.702±0.074	0.351±0.037
Reduced major axis	4.876±0.208	0.762±0.060	0.381±0.030
Mean OLS	4.978±0.211	0.791±0.060	0.396±0.030

Regression analysis between $\log v$ and $(\log h + b\mu_0)$ for the field galaxy data presented in Section 2 (excluding ESO-LV 1220040). The values x and y define the best-fitting plane such that $v \propto I_0^x h^y$ where $\mu_0 = -2.5\log I_0$. The TF relation is obtained when $b=-0.2$.

tively important distance errors for some of the more nearby galaxies due to streaming motions above the smooth Hubble flow. To address this concern, the regression analysis has been repeated excluding the 34 galaxies[8] within 3,000 km s^{-1}. The results obtained from the regression analysis of this data are fully consistent with the results from the larger galaxy sample, with $v \propto I_0^{0.53\pm0.06} h^{0.85\pm0.12}$ (B-band) and $v \propto I_0^{0.45\pm0.05} h^{0.75\pm0.13}$ (R-band). Additionally, correction for Virgo-infall alone, using the 220-model of Kraan-Korteweg (1986), gave entirely consistent results with those obtained using the more detailed velocity flow model of Burstein et al. (1989).

A meaningful comparison of the best-fitting planes for the early-type and late-type (>Sc) spiral galaxies in the present data set is not possible because the uncertainty on the exponents is in general too great. What we can, however, conclude at this point is that in the B-band, the near independency of M/L_B on surface brightness holds when the HSB galaxies are taken on their own, when the HSB and LSB galaxies are taken together, and when one constrains the 'mixing' value b to -0.2 in order to mimic the TF relation. Although, it is noted that this situation is expected to change in the redder passbands, where the slope of the TF relation is steeper (see section 5).

[8] Of the 5 galaxies identified previously as 'outliers' in Figure 1, only two of these are within this volume.

4.2 Does M/L_B correlate with $\mu_{0,B}$?

Two points can be made regarding previous B-band studies which have claimed, and even plotted, a trend between mass-to-light ratio and central disk surface brightness. The first point is addressed by plotting the present data. Figure 5a shows the 'kinematical' M/L_B ratio (equation 5) versus the central B-band disk surface brightness $\mu_{0,B}$. One can see that although an upper envelope appears to exist, the current data present no strong correlation between M/L_B and $\mu_{0,B}$. Furthermore, the upper envelope is merely a reflection of the upper (bright) envelope in the μ_0–$\log h$ diagram (Graham 2001b; Graham & de Blok 2001) which is due to the absence of large scale-length galaxies with bright disks. Panel b) in Figure 5 displays the data from Table 1 of McGaugh & de Blok (1998). Their tabulated circular velocities, B-band scale-lengths and central disk surface brightnesses were used to compute the kinematical mass-to-light ratio within four scalelengths. This was done in exactly the same way as for panel a) and is in fact the method claimed to

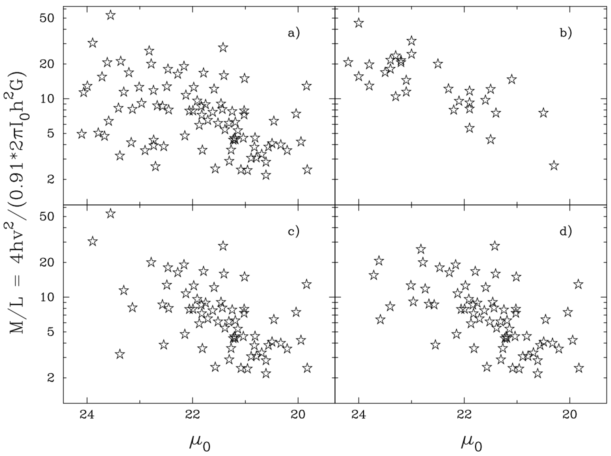

Figure 5. The kinematic M/L ratio (in solar units) is shown against the central disk surface brightness (B-band data). Panel a) contains the data described in Section 2, excluding the five outlying points identified in Figure 1. Panel b) shows the smaller data sample from Table 1 of McGaugh & de Blok (1998). Panel c) shows the data from panel a), excluding LSB galaxies with μ_0 fainter than 22.65 B-mag arcsec^{-2} and with h smaller than 8.45 kpc (see Section 4.2 for details). Panel d) shows the HSB galaxy sample from panel a) (excluding all three HSB galaxies with μ_0 fainter than 23.0 B-mag arcsec^{-2}) together with the LSB galaxies in common with McGaugh & de Blok (1998).

have been used in McGaugh & de Blok (1998). Strangely, their tabulated M/L ratios are different to the values derived from these basic parameters, and consequently their Figure 4b looks different to Figure 5b shown here. Although the upper envelope is common between panels a) and b), the lower-left portions differ significantly.

The disk-dominated LSB galaxies from de Blok et al. (1995) have roughly the same scale-lengths as normal HSB spiral galaxies – their median B-band scale-length is 4.3 kpc (H_0 = 75 km s^{-1} Mpc^{-1}; de Blok et al. 1995). The bulge-dominated LSB galaxies from Beijersbergen et al. (1999) have a larger median B-band disk scale-length of 12.6 kpc (Beijersbergen et al. 1999). Taking 8.45 kpc (=[12.6+4.3]/2) to represent some kind of division between the large and small (or rather, large and normal) sized LSB galaxies, panel c) shows the results after selecting against (i.e. excluding) those disks with central surface brightnesses more than one mag fainter than the canonical Freeman (1970) value of 21.65 B-mag and with scale-lengths less than 8.45 kpc. These galaxies should roughly have, on average, the same scale-lengths as the HSB galaxy sample, but fainter surface brightnesses. If the M/L ratio is independent of surface brightness, then we should find that we have removed those LSB galaxies with similar M/L ratios as the HSB galaxies - which indeed is what we do find. Panel d) shows the current HSB galaxy sample (excluding the three disks with μ_0 fainter than 23.0 B-mag arcsec^{-2}) together with those LSB galaxies in common with McGaugh & de Blok (1998). From this restricted sample, a somewhat similar correlation between M/L_B and $\mu_{0,B}$ to that present in the data of McGaugh & de Blok (1998) appears. *The dependence of the B-band mass-to-light ratio on the central disk surface brightness can therefore arise from ones sample selection, even with a range of disk luminosities*

McGaugh & de Blok (1998) excluded a number of LSB galaxies for a variety of different reasons. All of the LSB galaxies in common with both studies but excluded by McGaugh & de Blok (1998) (N = 7) reside very close to the mean relation defined by the other galaxies in Figure 1. That is, they do not appear to be outliers.

The second point which should however be mentioned is that in contradiction with most B-band TF studies, the small sample of McGaugh & de Blok (1998) apparently has a TF slope of almost 4, i.e. $x = 0.25$ (their Figure 1). In this case, as explained in Section 3, one does expect to find a strong correlation between M/L and μ_0, as these authors did for their galaxy sample.

5 LITERATURE COMPARISONS

A somewhat similar three-dimensional analysis of 511 HSB Spiral (and Irregular) galaxies having types Sa through Im has been performed by Burstein et al. (1997) in the B-band. While they also used rotational velocity estimates from W_{20} measurements, the nature of their photometric data is different to that used here. Using the RC3 (de Vaucouleurs et al. 1991) tables of B-band circular effective aperture size and mean enclosed surface brightness, Burstein et al. (1997) used the axial-ratio-based statistical relationships in the RC3 to derive the mean effective surface brightness $<\mu>_e = -2.5\log<I_e>$ within the effective radius r_e. They then corrected $<\mu>_e$ for Galactic extinction following Burstein & Heiles (1982) and for internal extinction using the correction 1.5log(b/a). Recognizing errors of more than 0.1 dex in their photometric parameters, Burstein et al. (1997) chose not to apply the small $(1+z)^4$ correction or any K-correction term. Their investigation effectively used the total (bulge + disk) galaxy half-light radius and mean surface brightness within this radius. Depending on the contribution of light from the bulge, varying fractions of disk scale-length, and hence the disks themselves, were consequently sampled in their analysis. The present investigation differs as it has used one complete disk scale-length and the central disk surface brightness; an approach, it should be noted, which effectively regards the bulge matter as dark matter - the luminous flux from the bulge is ignored, while the presence of the bulge permeates into the analysis through the rotational velocity of the disk.

If the relative contribution from the bulge light[9] is small enough that it can be neglected and the galaxy treated as simply an exponential disk, then the use of r_e and $<\mu>_e$ (or μ_e, the surface brightness at r_e) should yield similar results as the use of h and μ_0. This is because $r_e = 1.67h$ and $<\mu>_e = \mu_0 + 1.12$ ($\mu_e = \mu_0 + 1.82$) for an exponential disk. To investigate the influence of the bulge, and perform a somewhat more direct comparison with Burstein et al. (1997), the half-light radius and the surface brightness at this radius have been derived for the present galaxy sample and the fundamental plane recomputed using these values. The differences between the half-light radius of the disk (=1.67h) and the half-light radius of the galaxy (r_e),

[9] B/D ratios for much of the present galaxy sample have already been presented in Graham (2001a,b) and Graham & de Blok (2001).

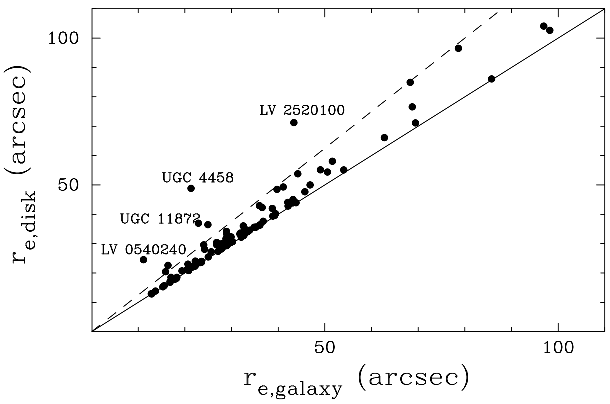

Figure 6. a) The B-band half-light radii of the disks ($r_{\rm e,disk} = 1.67h$) are plotted against the B-band half light radii of the galaxies ($r_{\rm e,galaxy}$). The presence of the bulge accounting for the differences. The dashed line denotes a 20 per cent difference from agreement (the solid line). The marked outliers have very prominent bulges within the half-light radius of the disk. b) The disk surface brightness at $r_{\rm e,disk}$ ($= \mu_0 + 1.82$) is plotted against the galaxy surface brightness at $r_{\rm e,galaxy}$.

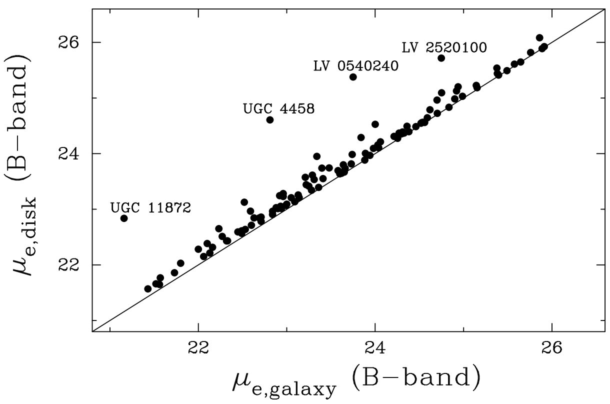

Figure 6 – *continued*

and the surface brightness of the disk at $1.67h$ and of the galaxy at r_e are shown in Figure 6. With the exception of a few galaxies[10] having very prominent bulges within their disk half-light radius, the disk and galaxy half-light radius usually varied by less than 20 per cent, and the surface brightness terms by less than $\sim$0.4 mag arcsec^{-2}. The optimal fundamental plane constructed using r_e and μ_e for the full sample (excluding the previously mentioned outliers) is $v \propto I_e^{0.53\pm0.05} r_e^{0.79\pm0.09}$ (B-band). For the HSB sample one finds $v \propto I_e^{0.61\pm0.11} r_e^{0.80\pm0.11}$, and for the LSB sample $v \propto I_e^{0.57\pm0.13} r_e^{0.87\pm0.17}$.

From the sample of 386 Sa-Sc Spiral galaxies analysed by Burstein et al. (1997), they found $v \propto < I >_e^{0.57\pm0.03} r_e^{0.85\pm0.05}$ (B-band). Applying the three-dimensional bisector regression analysis used in this paper to this very same data sample from Burstein et al. (1997) gives $v \propto < I >_e^{0.55\pm0.04} r_e^{0.78\pm0.05}$ (B-band). From equation 4 this implies that $(M/L_B) \propto < I >_e^{0.10\pm0.08} r_e^{0.56\pm0.10}$, in good agreement with the present papers investigation.

[10] These galaxies are not the outliers identified in Figure 1.

When Burstein et al. (1997) included all Spiral and Irregular galaxy types in their analysis, they found $v \propto < I >_e^{0.39\pm0.02} r_e^{0.61\pm0.02}$ (B-band), a result with notably lower exponents. Although, applying the three-dimensional bisector regression analysis gives $v \propto < I >_e^{0.41\pm0.01} r_e^{0.62\pm0.02}$, and excluding the Irregular type galaxies raises the exponents slightly to give $v \propto < I >_e^{0.44\pm0.02} r_e^{0.66\pm0.02}$ (B-band). When the same internal extinction correction as used by Burstein et al. (1997) is applied to this papers field galaxy sample, one obtains $v \propto I_e^{0.48\pm0.04} r_e^{0.73\pm0.07}$ (B-band), consistent at the 1σ level with the result from Burstein et al. (1997).

The result from Burstein et al. (1997), using all 511 disk galaxies and irregular galaxies, leads to (although not given in their paper) $L \propto v^{2.56\pm0.13} r_e^{0.44\pm0.07}$ (B-band). An even larger departure from the TF relation and dependence on a third parameter was found by Willick (1999) who derived $L \propto v^{2.4} r_e^{0.7}$ (R-band). Others have also previously found evidence for the residuals about the TF relation to correlate with a third parameter (Kodaira 1989; Salucci, Frenk & Persic 1993; Feast 1994; Theureau 1998; Koda et al. 2000a; Han et al. 2001, Kannappan et al. 2002), and it may be that the TF relation reflects closely, but not exactly, the Fundamental-Plane-like distributions shown here. However, there are numerous papers (e.g. Freudling 1990; Karachentsev 1991; Strauss & Willick 1995; Courteau 1997; and references therein) which, like this one, do not detect deviations above the 1-2σ level.

It should also be kept in mind that different papers have used different methods of regression analysis to fit a plane or line to their data points. Under the "clearly unrealistic" assumption of a constant M/L ratio, and minimising the residuals in luminosity, Shen, Mo & Shu (2002) derived the I-band relation $L_I \propto h^{0.50} v^{2.60}$ from theoretical expectations. This transforms into $v \propto I^{0.40} h^{0.60}$ - in remarkable agreement with this papers R-band result ($v \propto I^{0.43} h^{0.69}$). The present papers interest lies in deriving M/L ratio estimates which can be compared with theory. The disk parameters have consequently been treated equally when constructing the optimal plane; an approach which differs from the numerous direct and inverse TF relations constructed in the past for the determination of galaxy distances – which is not the subject of the current paper. A detailed comparison with every previous study is therefore not straight-forward if at all even possible. However, a detailed analysis of one other well-respected data sample shall be presented.

The reduced and tabulated photometric data of Tully et al. (1996) and the reduced kinematic data from Verheijen & Sancisi (2001) is analysed. This consists of B, R, I and K' scale-lengths and central disk surface brightnesses, obtained from marking the disk by eye, and rotational velocities taken from where the rotation curve is flat ($v_{\rm flat}$). The galaxy sample are all from the Ursa Major Cluster and consequently distance errors will not contribute quite as much to the scatter. For the sake of consistency, the surface brightness term has been uniformly corrected here in the same way as the previous data was dealt with (see Section 2). Because this new sample contains relatively edge-on Spiral galaxies, the K'-band inclination corrections to the central surface brightness terms are large, in some cases >2.0 mag arcsec^{-2}. For four galaxies which were catalogued to be completely edge-

Table 3. Regression Analysis: Cluster Galaxies

Band	x	y	M/L
B	0.396±0.059	0.732±0.118	$I_0^{-0.208\pm0.118} h^{0.464\pm0.236}$
R	0.334±0.035	0.642±0.098	$I_0^{-0.332\pm0.070} h^{0.284\pm0.196}$
I	0.303±0.029	0.601±0.092	$I_0^{-0.394\pm0.058} h^{0.202\pm0.184}$
K'	0.258±0.020	0.569±0.073	$I_0^{-0.484\pm0.040} h^{0.138\pm0.146}$

Three-dimensional bisector regression analysis between $\log v$, μ_0, and $\log h$ for Ursa Major Galaxy Cluster members. The exponents x and y define the best-fitting plane such that $v \propto I_0^x h^y$ where $\mu_0 = -2.5 \log I_0$. The photometric data (μ_0, h) comes from Tully et al. (1996) and the kinematic data (v) from Verheijen & Sancisi (2001).

on, their inclinations were set to 85° when calculating this correction.

The results of the three-dimensional bisector regression analysis are presented in Table 3. In the B-band, the analysis reveals that $\log(M/L_B) \propto (0.08\mu_0 + 0.46 \log h)$, in good agreement with the previous B-band results and revealing that changes in scale-length are more important than changes in surface brightness. Figure 7 shows the results for the K'-band data with $(C = 1.0)$ and without $(C = 0.0)$ the inclination correction ($2.5C \log[a/b]$, where a/b is the observed disk axis-ratio) to the surface brightness term. From the scatter one can clearly see that at near-infrared wavelengths, spiral galaxy disks should be taken to be transparent for such tests (see also Graham 2001b). One can see that the TF relation is obtained (i.e. $y \sim 2x$), and the slope increases from the B-band to the K'-band such that $L_B \propto v^{2.5}$ and $L_{K'} \propto v^{4.0}$. The reduction in scatter with increasing wavelength has also been observed for many years (Aaronson, Huchra & Mould 1979). Therefore, in the near-infrared, where one is affected little by obscuring dust and young stellar populations, the $M/L_{K'}$ ratio varies as $I_0^{-1/2}$, independent of h.

To again investigate possible differences between the mass-to-light ratios obtained using equation 4 and equation 5, and hence possible signatures that the total-mass profile does not scale linearly with the luminous disk profile, we have repeated Figure 4 this time using the Ursa Major galaxy Cluster data. Figure 8 presents the B-band analysis, which can be seen to display an identical behavior to that observed in Figure 4. This tends to suggest that the ratio of the mass-profile scale-size to the B-band disk scale-length may not be constant, but scales weakly with the B-band disk luminosity (see Section 3). Figure 9 shows the K'-band data where one can see that the weak B-band dependency on absolute magnitude ($r = 0.4$, Figure 8, lower panel) is reduced even further.

Lastly, it should perhaps also be noted that there is another mechanism to change the slope of the optimal plane within a given passband. Tully et al. (1998) have presented evidence that the appropriate extinction correction for disk galaxies in Clusters may be a function of galaxy luminosity. This was a subsequent paper to the Tully & Verheijen (1997) paper which addressed the issue of extinction corrections and provided the somewhat more standard corrections which have been used in this paper. Tully et al. (1998) analysed the data from two galaxy Clusters (53 galaxies from Ursa Major and 34 galaxies from Pisces) to determine a

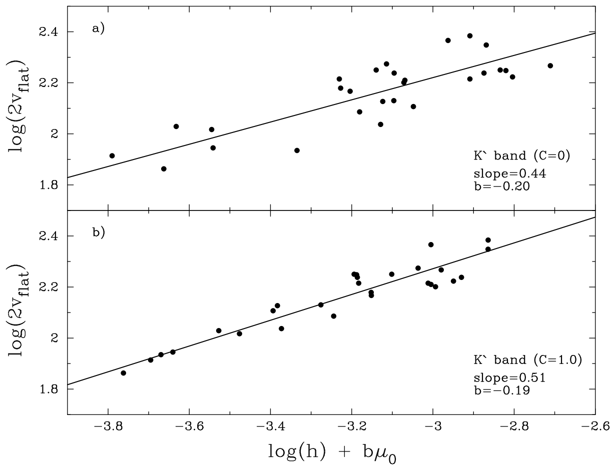

Figure 7. Orthogonal regression analysis to the K'-band data from Tully et al. (1996) and the velocity data from Verheijen & Sancisi (2001). The value of b was computed, as in Figure 1, such that it resulted in the highest linear correlation coefficient between $\log 2v_{\rm flat}$ and $(\log h + b\mu_0)$. When $b = 0.20$ these diagrams represent the TF relation, where $L \propto v^{2/{\rm slope}}$. The value of C dictates the apparent opacity of spiral galaxy disks for determinations of μ_0, such that the inclination correction to the surface brightness term μ_0 can be written as $2.5C \log(a/b)$, where a/b is the observed outer disk axis ratio. Panel a) assumes the disks are opaque $(C = 0)$, while panel b) assumes that they are fully transparent $(C = 1)$, resulting in considerably less scatter to the diagram.

TF slope of 3.1 in the B-band after applying their luminosity dependent extinction correction. This is an increase of 0.2 from 2.9 found by Sprayberry et al.'s (1995) study of the Ursa Major Cluster. Perhaps contrary to this, Willick et al. (1996) found no evidence for a luminosity-dependent extinction correction when using field galaxies. The interesting analysis by Tully et al. (1998) raises many questions. For instance, the data for the Pisces Cluster galaxies on their own appear to suggest no luminosity dependent extinction correction. Additionally, whether the results in Tully et al. (1998) can be extended to LSB galaxies is unclear; why an unevolved LSB galaxy with the same luminosity as a HSB galaxy should have the same amount of extinction due to dust is not obvious. Why the S0 and S0/a galaxies do not conform is a further mystery. The issue of corrections due to dust in field galaxies is not yet fully understood, or at least commonly accepted, and therefore it should be noted that the extinction corrections used here may need adjusting when this subject is on a firmer footing.

6 COLOURS

The $(B - R)$ colour of each galaxy's disk has been estimated using two approaches. Having previously modelled both the bulge and disk, we are better able to determine the $(B - R)$ colour for the disk alone - rather than the integrated colour of the bulge and disk. The first method has taken the difference between the corrected (see section 2) central disk surface brightness in B and R, and the second approach has used the difference between the total disk magnitude determined in the B and R passbands. Each galaxies dy-

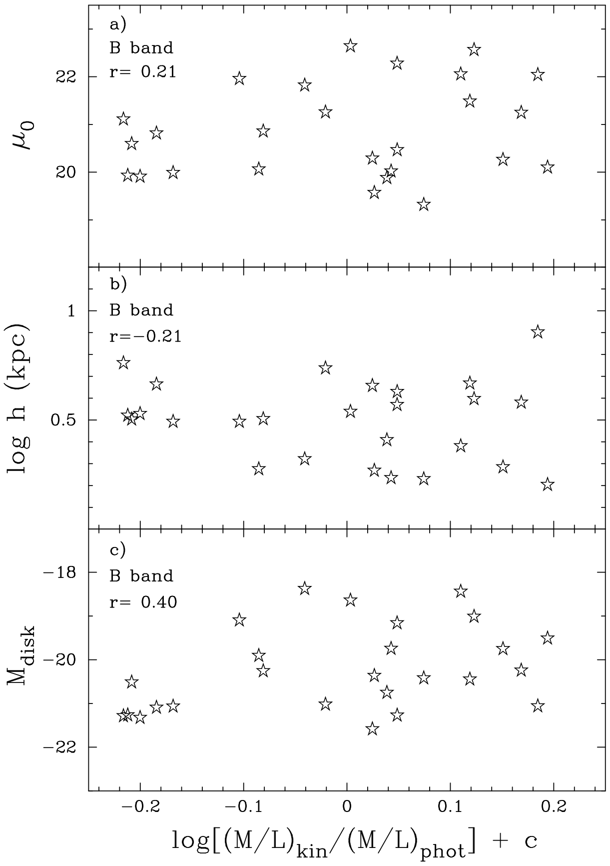

Figure 8. The logarithm of the difference between the mass-to-light ratio estimates obtained using equation 4 and equation 5 have been plotted against the central disk surface brightness (top panel), the logarithm of the disk scale-length (middle panel), and the absolute magnitude of the disk (bottom panel). These plots show the B-band data from Tully et al. (1996) and the velocity data from Verheijen & Sancisi (2001). The values for x and y used in equation 4 have been taken to be 0.396 and 0.732 (see Table 3). Constants of proportionality have been ignored, and the value of c in the x-axis is simply a constant.

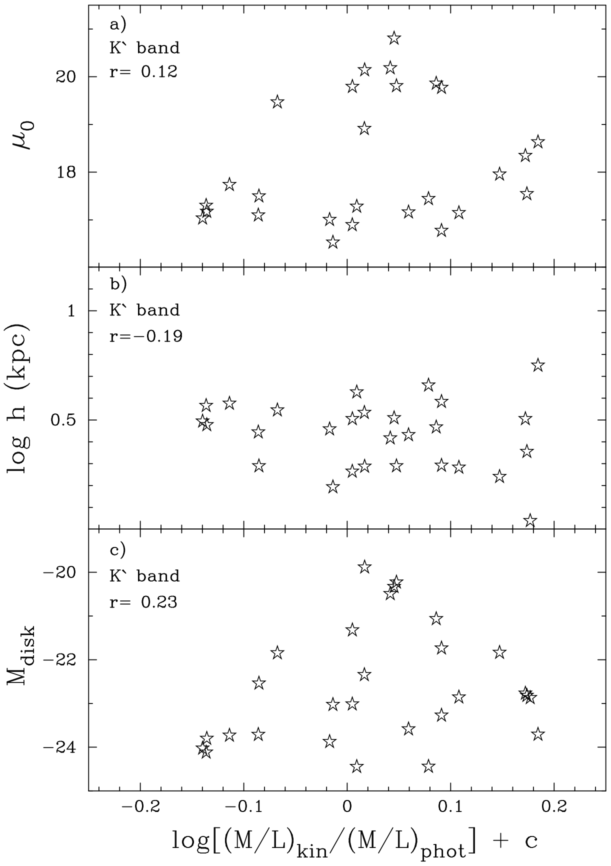

Figure 9. Same as Figure 8 but using K'-band data. The values for x and y used in equation 4 to derive $(M/L)_{\rm phot}$ have been taken to be 0.258 and 0.569.

namical mass-to-light ratio estimate (from equation 5) is plotted against its $B-R$ colour in Figure 10 for the HSB and LSB field galaxies, and in Figure 11 for the Ursa Major Cluster data from Tully et al. (1996) and Verheijen & Sancisi (2001). Only the disk light (that is, not the bulge light) has been used in this derivation of the dynamical mass-to-light ratio. Using the combined disk and bulge light to determine the mass-to-light ratio has very little effect on this result. It is immediately obvious that, within the noise of the present field galaxy data, no obvious correlation exists between the B- and R-band dynamical mass-to-light ratio and $B-R$ colour. An orthogonal regression analysis has been performed for those plots showing a possible correlation, and the Pearson correlation coefficient determined (results shown within the figures). In general, the correlations are weak.

Using a suite of simplified galaxy disk evolution models, Bell & de Jong (2001) have presented the case that the *stellar* mass-to-light ratio of the disk ($M_{*,\rm disk}/L_{\rm disk}$) should be correlated with colour. Their strongest correlation was obtained with the colour $(B-R)$ such that the logarithm of a disks B-band stellar mass-to-light ratio varies as $1.25(B-R)$. While the present paper has dealt with the dynamical, or total, mass-to-light ratio ($M_{\rm dyn}/L_{\rm disk}$) within a fixed number of disk scale-lengths (i.e. 4), one can combine the present observational results with the theoretical predictions of Bell & de Jong (2001) to determine how the stellar-to-dynamical[11] mass ratio must vary with $(B-R)$ colour.

The only strong correlation detected between the dynamical mass-to-light ratio and $(B-R)$ colour is in the K'-band data of the Cluster Spiral galaxies (Figure 11), where $\log(M_{\rm dyn}/L_{K'\rm disk}) \propto -1.25\pm0.28(B-R)$ (Figure 11). Combining this result with the stellar mass-to-light ratio prediction of Bell & de Jong (2001) ($\log[M_{*,\rm disk}/L_{K,\rm disk}] \propto 0.45[B-R]$), and neglecting differences between K and K', would imply that the logarithm of the stellar-to-dynamical mass ratio must increase as disks become redder, varying as $1.70\pm0.28(B-R)$. If the theoretical models are correct, *this implies that galaxy modellers should not assume a constant stellar-to-total mass ratio (at least within 4h) for any given passband.* This conclusion seems to be at least qualitatively correct; LSB galaxies are largely unevolved blue galaxies

[11] By stellar-to-dynamical mass ratio, it is meant the ratio of the stellar disk mass (excluding any possible bulge mass) to the total dynamical mass within 4 scale-lengths.

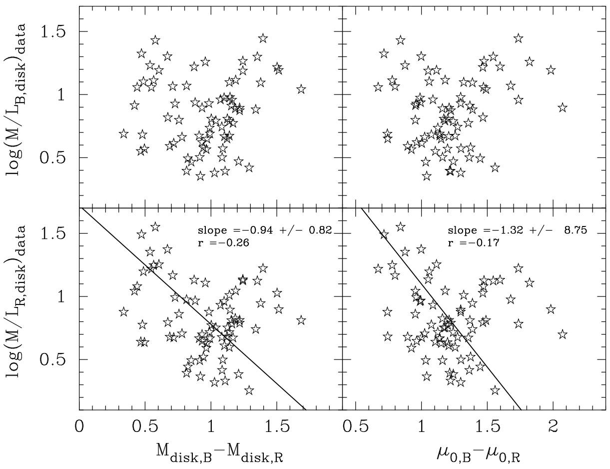

Figure 10. The logarithm of the dynamical mass-to-light ratio obtained using equation 1 (with $r = 4h$) is plotted against two measures of the disk colour ($B - R$). The left hand column shows the colour difference between the integrated disk magnitude in B and R, while the right hand column shows the difference between the central disk surface brightness in B and R. Only the disk luminosity (not the bulge and disk luminosity) has been used to derive the mass-to-light ratio, which is given here in solar units. An orthogonal regression analysis has been used to derive the slope (and error) to the correlation, and the Pearson correlation coefficient is also given for those plots displaying a possible correlation.

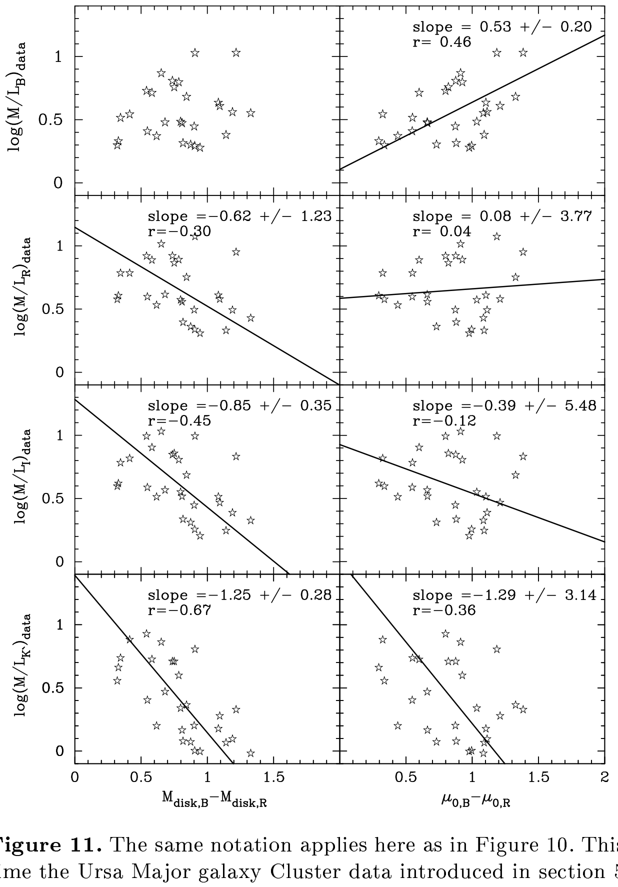

Figure 11. The same notation applies here as in Figure 10. This time the Ursa Major galaxy Cluster data introduced in section 5 has been used.

with higher relative gas-to-total mass fractions than HSB galaxies (Bothun, Impey & McGaugh 1997).

7 CONCLUSIONS

The best-fitting two-dimensional plane to the 3-dimensional space of galaxy disk parameters (rotational velocity $v_{\rm rot}$, disk scale-length h, and central disk surface brightness $\mu_0 = -2.5 \log I_0$) has been derived for a sample of nearly 100 field galaxies. In the B-band $v_{\rm rot} \propto I_0^{0.50\pm0.05} h^{0.77\pm0.07}$, and in the R-band $v_{\rm rot} \propto I_0^{0.43\pm0.04} h^{0.69\pm0.07}$. This implies that in the B-band the dynamical M/L ratio is, contrary to popular claims, nearly independent of the disk surface brightness level; the disk scale-length is what is important, with $\log(M/L_B) \propto 0.00(\pm0.04)\mu_0 + 0.54(\pm0.14) \log h$. This general result holds when using HSB field galaxies, when using HSB and LSB field galaxies together, and when derived from the TF relation instead of the best-fitting two-dimensional plane. We should therefore not talk simply about LSB and HSB galaxies, but also give mention to their scale-lengths.

The M/L_B ratio is shown to be largely independent of a disks ($B - R$) colour, whereas M/L'_K varies as -1.25±0.28($B - R$). Combining this with recent theoretical modelling implies that the logarithm of the stellar-to-dynamical mass ratio is not a constant value, but increases as disks become redder, varying as 1.70±0.28($B-R$). Consequently, galaxy modellers should not treat this as a constant quantity.

In the R-band $\log(M/L_R) \propto 0.06(\pm0.03)\mu_0 + 0.38(\pm0.14) \log h$. Extensions to redder passbands, albeit using a sample of Cluster spirals, reveals that the M/L ratio becomes increasingly less dependent on the disk scale-length at longer wavelengths, reaching the situation where $M/L \propto 1/\sqrt{I_0}$ at K'.

Marginal evidence is presented to suggest that the ratio of the mass-profile scale-size (a) to the luminous disk scale-length (h) may vary with disk luminosity in the B-band, such that a/h decreases with increasing disk luminosity. A method to test this tentative possibility is described.

8 ACKNOWLEDGEMENTS

I wish to thank Erwin de Blok for kindly providing me with electronic tables of the kinematical data used in this study. I am also grateful to David Burstein and Renée Kraan-Korteweg for providing me with their velocity flow codes, and to Bahram Mobasher and Ken Freeman for their careful reading and helpful comments on this manuscript.

This research has made use of the LEDA database (http://leda.univ-lyon1.fr). This research has made use of the NASA/IPAC Extragalactic Database (NED) which is operated by the Jet Propulsion Laboratory, California Institute of Technology, under contract with the National Aeronautics and Space Administration. The Parkes telescope is part of the Australia Telescope which is funded by the Commonwealth of Australia for operation as a National Facility managed by CSIRO.

REFERENCES

Aaronson M., Huchra J., Mould J., 1979, ApJ, 229, 1

Andersen D.R., Bershady M.A., Sparke L.S., Gallagher J.S., Wilcots E.M., 2001, ApJ, 551, L131

Barnes D.G., et al., 2001, MNRAS, 322, 486

Beijersbergen M., de Blok W.J.G., van der Hulst J.M., 1999, A&A, 351, 903

Bell E.F., de Jong R.S., 2001, ApJ, 550, 212

Bothun G.D., Impey C.D., McGaugh S.S., 1997, PASP, 109, 745

Bouwens R., Silk J., 2002, ApJ, 568, 522

Burkholder V., Impey C., Sprayberry D., 2001, AJ, 122, 2318

Burstein D., Bender R., Faber S.M., Nolthenius R., 1997, AJ, 114, 1365

Burstein D., Davies R.L., Dressler A., Faber S.M., Lynden-Bell D., 1989, in Large scale structure and motions in the universe, Mezetti, M., ed., Dordrecht, Kluwer Academic Publishers, p.179

Caon N., Capaccioli M., D'Onofrio M., 1993, MNRAS, 265, 1013

Dalcanton J.J., Spergel D.N., Summers F.J., 1997, ApJ, 482, 659

de Blok W.J.G., McGaugh S.S., 1997, MNRAS, 290, 533

de Blok W.J.G., McGaugh S.S., Rubin V.C., 2001, ApJ, in press

de Blok W.J.G., McGaugh S.S., van der Hulst J.M., 1996, MNRAS, 283, 18

de Blok W.J.G., van der Hulst J.M., Bothun G.D., 1995, MNRAS, 274, 235

Courteau S., 1997, AJ, 114, 2402

de Jong R.S., 1996, A&AS, 118, 557

de Jong R.S., van der Kruit P.C., 1994, A&AS, 106, 451

de Vaucouleurs G., de Vaucouleurs A., Corwin H.G., Buta R.J., Paturel G., Fouque P., 1991, Third Reference Catalog of Bright Galaxies (Springer-Verlag, New York)(RC3)

Djorgovski S., Davis M., 1987, ApJ, 313, 59

Dressler A., Lynden-Bell D., Burstein D., Davies R.L., Faber S.M., Terlevich R.J., Wegner G., 1987, ApJ, 313, 42

Faber S.M., Jackson R.E., 1976, ApJ, 204, 668

Faber S.M., Dressler A., Davies R.L., Burstein D., Lynden-Bell D., Terlevich R.J., Wegner G., 1987, in Faber S.M., ed., Nearly Normal Galaxies, Springer, New York, p.175

Fall S.M., 2002, in The Dynamics, Structure and History of Galaxies (Kenneth Freeman 60th Birthday Conference), eds. G.S. Da Costa & E.M. Sadler, astro-ph/0203492

Feast M.W., 1994, MNRAS, 266, 255

Feigelson E.D., Babu G.J., 1992, ApJ, 397, 55

Franx M., de Zeeuw T., 1992, ApJ, 392, L47

Freeman K.C., 1970, ApJ, 160, 811

Freudling W., 1990, A Search for streaming motion around the Hercules Void, Ph.D. Thesis, Cornell Univ.

Giovanardi C., Hunt L.K., 1988, AJ, 95, 408

Graham A.W., 2001a, AJ, 121, 820

Graham A.W., 2001b, MNRAS, in press

Graham A.W., Colless M.M., 1997, MNRAS, 287, 221

Graham A.W., de Blok W.J.G., 2001, ApJ, 556, 177

Han J.L., Deng Z.G., Zou Z.L., Wu X.B., Jing Y.P., 2001, PASJ, 53, 853

Haynes M.P., van Zee L., Hogg D.E., Roberts M.S., Maddalena R.J., 1998, AJ, 115, 62

Huchtmeier W.K., Karachentsev I.D., Karachentseva V.E., Ehle M., 2000, A&AS, 141, 469

Isobe T., Feigelson E.D., Akritas M.G., Babu G.J., 1990, ApJ, 364, 104

Kannappan S.J, Fabricant D.G., Franx M., 2002, AJ, in press (astro-ph/0202111)

Karachentsev I.D., 1991, Soviet Astron. Lett., 17, 283

Koda J., Sofue Y., Wada K., 2000a, ApJL, 531, L17

Koda J., Sofue Y., Wada K., 2000b, ApJ, 532, 214

Kodaira K., 1989, ApJ, 342, 122

Kraan-Korteweg R.C., 1986, A&AS, 66, 255

Kravtsov A.V., Klypin A., Bullock J.S., Primack J.R., 1998, ApJ, 502, 48

Lauberts A., Valentijn E.A., 1989, The Surface Photometry Catalogue of the ESO-Uppsala Galaxies (ESO-LV). European Southern Observatory

Lynden-Bell D., Faber S.M., Burstein D., Davies R.L., Dressler A., Terlevich R.J., Wegner G., 1988, ApJ, 326, 19

Matthews L.D., Gallagher J.S., ApJS, in press (astro-ph/0203188)

Mo H.J., Mao S., 2000, MNRAS, 318, 163

Mo H.J., Mao S., White S.D.M., 1998, MNRAS, 295, 319

McGaugh S.S., Schombert J.M., Bothun G.D., de Blok W.J.G., 1999, ApJ, 533, L99

McGaugh S.S., de Blok W.J.G., 1998, ApJ, 499, 41

Navarro J.F., Frenk C.S., White S.D.M., 1996, ApJ, 462, 563

Persic M., Salucci P., 1991, 368, 60

Poggianti B.M., 1997, A&AS, 122, 399

Richter O.-G., Sancisi R., 1994, A&A, 290, 9

Rubin V.C., Burstein D., Ford W.K.Jr., Thonnard N., 1985, ApJ, 289, 81

Salucci P., Ashman K.M., Persic M., 1991, ApJ, 379, 89

Salucci P., Borriello A., 2002, 8th Adriatic Meeting: Particle Physics in the New Millennium, Lecture Notes in Physics, Springer Verlag (astro-ph/0203457)

Salucci P., Frenk C.-S., Persic M., 1993, MNRAS, 262, 392

Schlegel D.J., Finkbeiner D.P., Davis M., 1998, ApJ, 500, 525

Schombert J.M., Bothun G.D., 1988, AJ, 95, 1389

Schombert J.M., Bothun G.D., Schneider S.E., McGaugh S.S., 1992, AJ, 103, 1107

Sèrsic J.-L., 1968, Atlas de Galaxias Australes (Cordoba: Observatorio Astronomico)

Shen S., Mo H.J., Shu C., 2002, MNRAS, 331, 259

Strauss M.A., Willick J.A., 1995, Phys. Rep., 261, 271

Swaters R.A., Madore B.F., Trewhella M., 2000, ApJ, 531, L107

Theureau G., 1998, A&S, 331, 1

Triay R., Lachieze-Rey M., Rauzy S., 1994, A&A, 289, 19

Tully R.B., Fisher J.R., 1977, A&A, 54, 661

Tully R.B., Fouqué, P., 1985, ApJS, 58, 67

Tully R.B., Pierce M.J., Jia-Sheng H., Saunders W., Verheijen M.A.W., Witchalls P.L., 1998, AJ, 115, 2264

Tully R.B., Verheijen M.A.W., Pierce M.J., Jia-Sheng H., Wainscoat R.J., 1996, AJ, 112, 2471

Tully R.B., Verheijen M.A.W., 1997, ApJ, 484, 145

van den Bosch, F.C., 2000, ApJ, 530, 177

van den Bosch, F.C., Robertson B.E., Dalcanton J.J., de Blok W.J.G., 2000, AJ, 119, 1579

van der Hulst J.M., Skillman E.D., Smith T.R., Bothun G.D., McGaugh S., de Blok W.J.G., 1993, AJ, 106, 548

Verheijen M.A.W., Sancisi R., 2001, A&A, in press (astro-ph 0101404)

Willick J.A., 1999, ApJ, 516, 47

Willick J.A., Courteau S., Faber S.M., Burstein D., Dekel A., Kolatt T., 1996, ApJ, 457, 460

Willick J.A., Courteau S., Faber S.M., Burstein D., Dekel A., Strauss M.A., 1997, ApJS, 109, 333

Zwaan M.A., van der Hulst J.M., de Blok W.J.G., McGaugh S.S., 1995, MNRAS, 273, L35